CORRIGENDUM

Development 135, 3623 (2008) doi:10.1242/dev.030817

Distinct cellular and molecular mechanisms mediate initial axon development and adult-stage axon regeneration in *C. elegans*

Christopher V. Gabel, Faustine Antoine, Chiou-Fen Chuang, Aravinthan D. T. Samuel and Chieh Chang

There was an error published in *Development* **135**, 1129-1136.

The name of author Faustine Antoine was misspelt and appears correctly above.

The authors apologise to readers for this mistake.

Development 135, 1129-1136 (2008) doi:10.1242/dev.013995

Distinct cellular and molecular mechanisms mediate initial axon development and adult-stage axon regeneration in *C. elegans*

Christopher V. Gabel[1], Faustine Antonie[2], Chiou-Fen Chuang[3], Aravinthan D. T. Samuel[1,*] and Chieh Chang[2,*]

The molecular and cellular mechanisms that allow adult-stage neurons to regenerate following damage are poorly understood. Recently, axons of motoneurons and mechanosensory neurons in adult *C. elegans* were found to regrow after being snipped by femtosecond laser ablation. Here, we explore the molecular determinants of adult-stage axon regeneration using the AVM mechanosensory neurons. The first step in AVM axon development is a pioneer axonal projection from the cell body to the ventral nerve cord. We show that regeneration of the AVM axon to the ventral nerve cord lacks the deterministic precision of initial axon development, requiring competition and pruning of unwanted axon branches. Nevertheless, axons of injured AVM neurons regrow to the ventral nerve cord with over 60% reliability in adult animals. In addition, in contrast to initial development, axon guidance during regeneration becomes heavily dependent on cytoplasmic protein MIG-10/Lamellipodin but independent of UNC-129/TGF-β repellent and UNC-40/DCC receptor, and axon growth during regeneration becomes heavily dependent on UNC-34/Ena and CED-10/Rac actin regulators. Thus, *C. elegans* may be used as a genetic system to characterize novel cellular and molecular mechanisms underlying adult-stage nervous system regeneration.

KEY WORDS: *C. elegans*, Femtosecond laser axotomy, Regeneration

INTRODUCTION

The nematode *C. elegans* has a simple and stereotyped nervous system, containing 302 neurons with a nearly complete map of all axons and synapses (White et al., 1986). As an accessible genetic model, *C. elegans* has long been used to identify and characterize molecules that affect axon growth and guidance during initial development. Recently, Yanik et al. and Wu et al. (Yanik et al., 2004; Wu et al., 2007) discovered that specific axons in *C. elegans* are capable of regenerating after adult-stage damage. Using femtosecond laser ablation, a new optical scalpel that exhibits submicrometer precision, Yanik et al. snipped the axons of GABAergic DD/VD motoneurons in adult *C. elegans* and discovered functional regeneration: snipping the axons abolished motility, but worms regained motility within 24 hours and displayed new axonal outgrowths, explaining the restoration of motility. Wu et al. found that the axons of the ALM and PLM mechanosensory neurons in *C. elegans* also regenerate after axotomy, but that regeneration after injury at the adult stage can display significant guidance errors. Wu et al. found that regenerative growth exhibits fewer guidance errors in larval animals, as well as in adult animals lacking the VAB-1 Eph receptor tyrosine kinase, suggesting that age may alter the molecular requirements for axon growth and guidance.

In this study, we extend femtosecond laser ablation to different neuronal types in *C. elegans*. We show that different neurons have different capacities for adult-stage regeneration. In particular, we discovered that the AVM mechanosensory neuron displays robust axon regeneration after adult-stage injury. The molecular requirements for initial axon development in the AVM mechanosensory neurons are particularly well understood, providing an opportunity for detailed analysis of the molecular differences for regenerative axon growth and guidance. AVM integrates both netrin- and slit-based cues to make its first decision in early development: a pioneer axonal projection from the cell body to the ventral nerve cord. During development, *unc-6*/netrin is expressed in ventral nerve cord neurons (Wadsworth et al., 1996), and *unc-40*/DCC is the netrin receptor that mediates ventral attraction of the developing AVM axon (Hao et al., 2001). During development, the dorsal body wall muscles express repellent *slt-1*, which facilitates dorsal repulsion of the developing AVM axon through the *sax-3*/ROBO receptors. By systematically comparing patterns in AVM axon regeneration in wild-type animals versus mutants with specific defects in the netrin and slit pathways, we establish distinct molecular requirements between initial axon development and adult-stage regeneration. Our observations show that *C. elegans* may be used to identify and characterize novel cellular and molecular mechanisms that mediate adult-stage axon regeneration.

MATERIALS AND METHODS

Strains

Nematodes were cultivated using standard protocols and maintained at 20°C (Brenner, 1974). The following mutations and transgenes were used: LGI, *unc-40(e1430), zdIs5[mec-4::gfp, lin-15(+)]*; LGIII, *mig-10(ct41)*; LGIV, *ced-10(n1993), unc-129(ev557), unc-5(e53), evIs82[unc-129::gfp, pMH86], kyIs179[unc-86::gfp]*; and LGV, *unc-34(gm104), oyIs14[sra-6::gfp, lin-15(+)], kyIs174[slt-1::gfp]*; LGX, *slt-1(eh15), sax-3(ky123), unc-6(ev400); oyIs144[odr-1::dsred]*.

Molecular biology

Standard molecular biology techniques were used. To study adult-stage expression of TGF-β, *unc-129p::YFP* was made by cloning the 3.5 kb *unc-129* promoter into pSM-YFP vector. Primers were designed with *Sph*I (5′) to *Bam*HI (3′) to amplify the *unc-129* promoter and clone into corresponding

[1]Department of Physics and Center for Brain Science, Harvard University, Cambridge, MA 02138, USA. [2]Department of Biology and Department of Neurology and Neurosurgery, McGill University, Montreal, Quebec H3A 1B1, Canada. [3]Division of Developmental Biology, Cincinnati Children's Hospital Medical Center, Cincinnati, OH 45229, USA.

*Authors for correspondence (e-mails: chieh.chang@mcgill.ca; samuel@physics.harvard.edu)

Accepted 2 January 2008

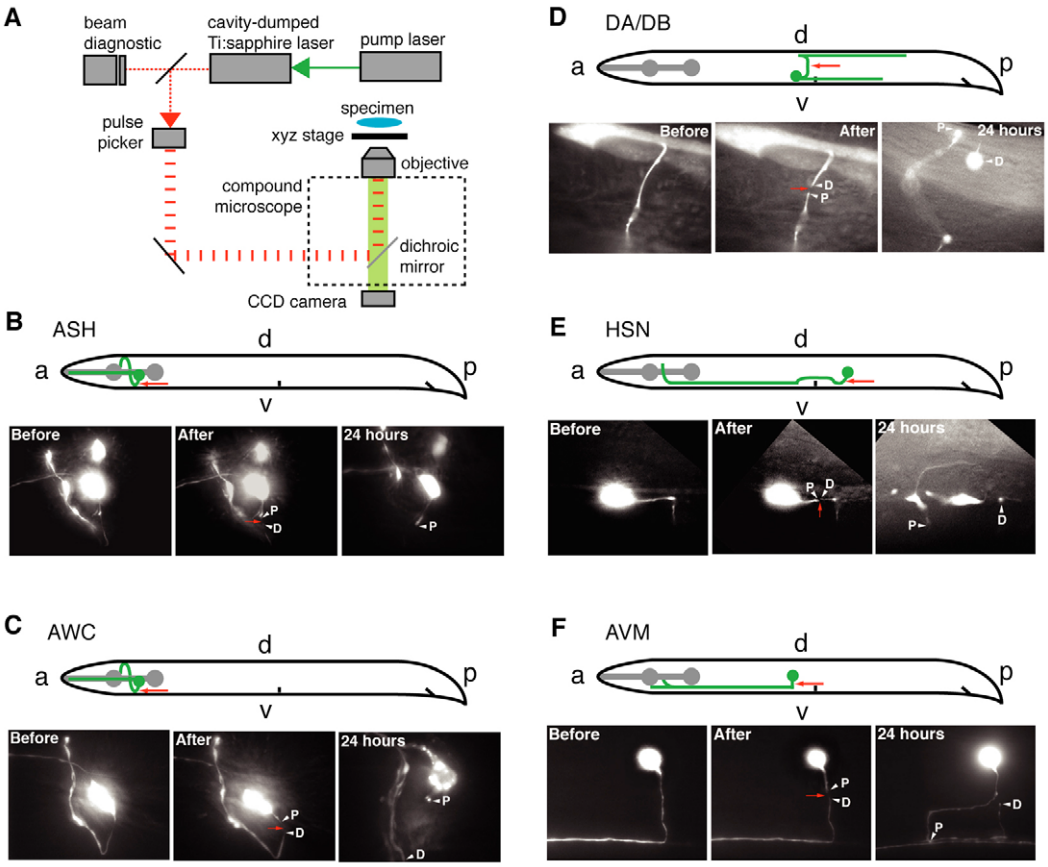

Fig. 1. Axon regeneration is exhibited by specific neuronal types. (**A**) Schematic of femtosecond laser system. (**B-F**) Axon trajectories of ASH, AWC, DA/DB, HSN and AVM neurons. In each case, an image is shown before, immediately after and 24 hours after surgery. D indicates the distal end and P the proximal end of severed axons. Red arrows point to the laser target. ASH and AWC axons were snipped at their posterior ventral projections; ASH axons did not noticeably grow out after 24 hours (B; *n=12*); AWC axons did not grow out at all (C; *n=12*). Representative examples of successful axon regeneration in the cholinergic DA/DB motoneurons (D), serotonergic HSN motoneurons (E) and AVM mechanosensory neurons (F).

sites in pSM-YFP. The *mec-4p::unc-34* and *mec-4p::ced-10* constructs were made by cloning *unc-34* or *ced-10* cDNA into *Kpn*I (5′) and *Spe*I (3′) sites in *pPD95.81* downstream of the *mec-4* promoter.

Transgenic animals

Germline transformation of *C. elegans* was performed using standard techniques (Mello and Fire, 1995). For example, the *unc-129::YFP* promoter fusion was injected at 50 ng/μl along with the co-injection marker *odr-1::gfp* at 40 ng/μl. Transgenic lines were maintained by following *odr-1::gfp* fluorescence. Other transgenes maintained as extrachromosomal arrays included: *xnEx84[mec-4::unc-34, odr-1::gfp]*, *xnEx86[mec-4::ced-10, odr-1::gfp]* and *cyEx21[mec-7::mig-10a, odr-1::dsred]*. The *mec-4::unc-34*, *mec-4::ced-10* and *mec-7::mig-10* were injected at 50 ng/μl along with the co-injection marker *odr-1::gfp* or *odr-1::dsred* at 40 ng/μl.

Laser surgery

Our femtosecond laser set-up is shown in Fig. 1A. We used a cavity-dumped Ti:sapphire laser oscillator (Cascade Laser, KMLabs, Boulder, CO) to generate ~100 fs laser pulses (Clark et al., 2006). The laser output was pruned to a 1 kHz pulse train by an Eclipse Pulse Picker (KMLabs Inc., Boulder, CO), which was tightly focused onto targets using a Nikon 100×, 1.4 NA oil-immersion objective. The vaporization threshold corresponds to pulse energies of 5-15 nJ (Shen et al., 2005; Chung et al., 2006). Successful axotomy was confirmed by visualizing targets immediately after exposure.

Microscopy

Neuronal morphology was based on high-magnification *z*-stacks using a Nikon TE2000 fluorescence microscope. We mounted worms on 2% agar pads containing 3 mM sodium azide, and imaged targeted neurons before and after axotomy. Worms were recovered from sodium azide, placed on fresh plates with bacterial foods, and reimaged after 24 hours. For time-lapse studies, we paralyzed worms with 0.05% tetramisole (Knobel et al., 1999), mounted them on 2% agar pads, sealed under cover glass and wax, and captured *z*-stacks every 15 or 30 minutes for 15 hours. The images presented in the figures were created from a maximum intensity projection of the corresponding *z*-stack. In some cases, individual planes of the *z*-stacks were modified to heighten the contrast and visibility of axonal processes.

Quantifying axon length after AVM regeneration

The axon length of regenerating neurons was quantified 24 hours after surgery. To produce the scatter plots in Fig. 5C and Fig. 7A, we scored the relative position of all axon termini from the dorsal and ventral midlines and AVM cell body. Owing to the curvature of the worm's body, two-dimensional projections of each *z*-stack would underestimate axon length. Therefore, we used image analysis software (MatLAB, Mathworks, Natick, MA) to effectively unroll the worm's cylindrical surface, quantifying anteroposterior distances using the coordinate parallel to the body centerline and dorsoventral distances along the cylindrical surface. *P* values for the ventral scores were calculated using a Chi-square test for equality of distributions. Axon lengths (Fig. 5E, Fig. 7C,D) were calculated as the actual contour length between the cell body and axon termini, by tracing the axon through a three-dimensional image stack. *P* values for the length measurements were calculated using a Student's *t*-test.

RESULTS

Different neuronal types have different capacities for adult-stage axon regeneration

Yanik et al. discovered functional regeneration of axons of the DA/DB motoneurons after adult-stage axotomy (Yanik et al., 2004). Wu et al. established that axons of the ALM and PLM mechanosensory neurons, as well as sensory dendrites of the AWB chemosensory neuron, can regenerate after adult-stage injury (Wu et al., 2007). We began the present study by examining regenerative ability in additional types of *C. elegans* neurons after femtosecond laser axotomy in young adult animals, within a few hours after the animals exited the last larval molt (Fig. 1). We found that axons of

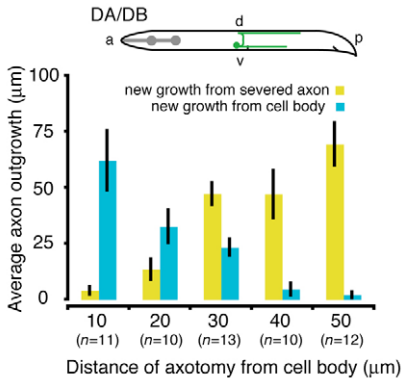

Fig. 2. Proximity of the axotomy point affects the manner of axon regeneration in DA/DB neurons. DA/DB motoneurons were cut at defined distances from the cell body. The total contour length of new outgrowth from the neuron was measured 24 hours after surgery and binned into two categories: continuing growth from the proximal end of the severed axon or new growth initiated at the cell body. Error bars represent ±1 s.e.m.

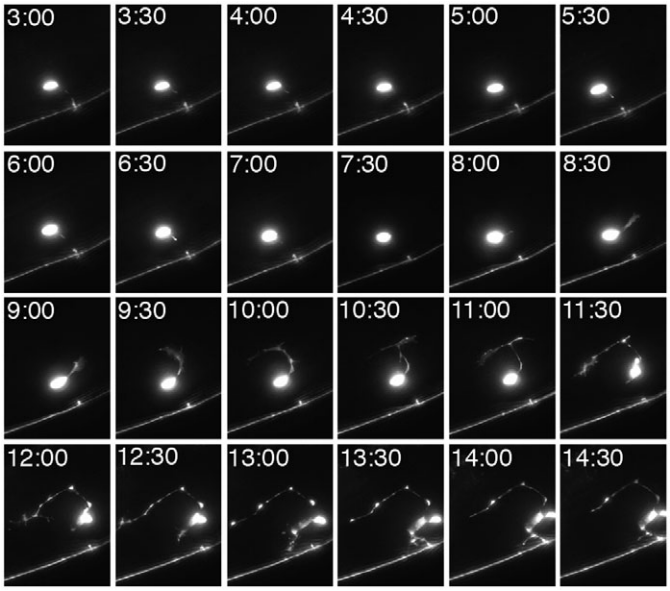

Fig. 3. Spatiotemporal dynamics of regenerative axon growth. Representative patterns in axon regeneration are shown with this mechanosensory neuron, imaged at 30-minute intervals for 15 hours following femtosecond laser axotomy using fluorescence microscopy. The dorsal and anterior directions are upwards and leftwards, respectively.

the ASH and AWC sensory neurons in the nerve ring within the head typically do not regenerate after adult-stage axotomy (Fig. 1B,C). By contrast, axons of AVM mechanosensory neurons and DA/DB and HSN motoneurons outside the nerve ring typically regenerate within 24 hours (Figs 1D-F). Thus, different neuronal types in *C. elegans* appear to exhibit different levels of regenerative ability.

After axotomy, regenerating axons either emerge from the cell body or as a continuation of the proximal end of the severed axon. We found that the manner of the regenerative growth depends on the proximity of the injury to the cell body. We quantified this effect by systematically cutting the axons of DA/DB motoneurons at precise distances from their cell bodies ranging from 10 μm to 50 μm (Fig. 2). When the injury is less than 30 μm from the cell body, new axons tend to emerge from the cell body. When the injury is 30 μm or more away, the regenerating axons tend to be continuations of the proximal end.

Similar observations have been made previously in immature hippocampal and cortical neurons (Dotti and Banker, 1987; Goslin and Banker, 1989; Hayashi et al., 2002; Bradke and Dotti, 2000). When hippocampal neurons are cultured in vitro after being dissociated from the embryonic brain, they reproducibly establish a single axon and several dendrites, despite the absence of environmental cues. The regeneration pattern is similarly dependent on the location of the axotomy with respect to the cell body. The severed axon will regrow from the proximal end if the cut is farther away from the cell body and the remaining axon stump is longer than 35 μm, while one of the neurites (dendrites) will grow out to become the new axon if the cut is close to the cell body and the remaining stump is shorter (Goslin and Banker, 1989). One possibility is that, upon cell-body distal axotomy, greater amount of a regulatory factor in the remaining axon stump can prevent other parts of the neuron from producing new axons.

Axon regeneration at the adult stage involves exploratory outgrowth and pruning

Differences in regenerative ability between different types of neurons may depend on intrinsic factors or on local cellular environment (Case and Tessier-Lavigne, 2005). In the present study, we focused on the AVM mechanosensory neuron, which has proven to be a particularly useful system for analyzing the molecular requirements for axon growth and guidance during initial development.

First, we explored the spatiotemporal dynamics of regeneration using time-lapse imaging after femtosecond laser axotomy, and identified distinct cell biological changes that characterize adult-stage axon regeneration. The cell body of an injured neuron sends out fanlike, lamellipodial growth cones. Multiple axons may be initiated from the injured neuron but not every axon reaches its target. Unwanted axons are pruned, suggesting a process of axon competition. In a representative series of time-lapse images (Fig. 3), the cell body of an injured mechanosensory neuron sent its first axon in the dorsal direction. Successive branches from the first axon failed to approach the ventral nerve cord. After persistent failure by the first axon, the cell body initiated a second axon in the ventral direction. After the second axon successfully reached the ventral nerve cord, the first axon began to retract. Some excess axons were not completely removed even after 24 hours. Although our results do not directly prove axon competition between regenerating axons, they are consistent with a competition model, which might provide an alternative explanation to the discovery by Wu et al. (Wu et al., 2007) of an inhibitory role of a synaptic branch on PLM regeneration. Wu et al. discovered that PLM axons cut distal to the ventral branch point typically do not regrow, but can regrow if the ventral branch is also severed. One possibility is that a regulatory cue from the ventral branch can signal to the PLM cell body to either prevent axon regrowth or promote axon pruning. Our time-lapse imaging enabled us to identify intermediate structures during mechanosensory axon regeneration, which seem to support a model in which the stabilization of one axon might cause the retraction of the other axon.

Wu et al. (Wu et al., 2007) found that regeneration of ALM and PLM mechanosensory neurons after axotomy at larval stages tends to exhibit fewer guidance errors than regeneration after axotomy at the

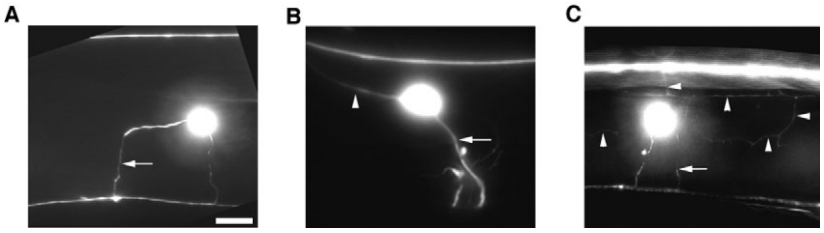

Fig. 4. Excess axons remain 24 hours after laser axotomy. (**A**) A representative example of an injured neuron with only a primary axon 24 hours after surgery. (**B**) An injured neuron with an ectopic axon from the cell body 24 hours after surgery. (**C**) Excessive axon sprouting from an injured neuron 24 hours after surgery. Arrows indicate primary axons and arrowheads denote ectopic axons. Scale bar: 20 μm.

adult stage. Our time-lapse imaging analysis shows that regenerating axons at the adult stage lack the deterministic precision of initial axon development. Although we were unable to perform the same time-lapse imaging to monitor initial axon development in the AVM neurons, as our fluorescence marker (*mec-4p::GFP*) only becomes visible in the AVM axon after its development is completed, we have several observations suggesting that initial wiring during larval development is rather precise. First, axon morphology after regeneration is highly variable, whereas axon morphology after development is stereotyped and practically indistinguishable from worm to worm (based on inspection of more than 100 wild-type worms). Second, pruning of unwanted axons in adult worms is often imperfect and excess axon outgrowths are commonly observed (Fig. 4), whereas we have never observed excess axon outgrowths after initial development. Finally, we were able to compare the effects of different developmental ages on the extent of AVM axon regeneration

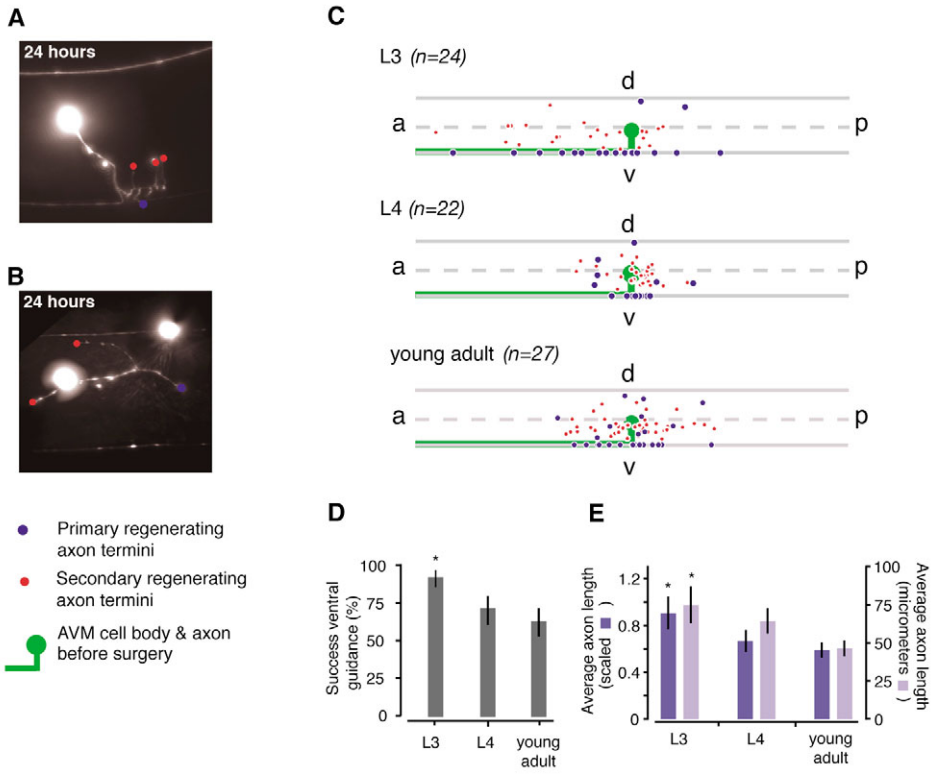

Fig. 5. Developmental stage affects axon regeneration. (**A**,**B**) Representative images showing the morphology of successful and unsuccessful AVM axon regeneration 24 hours after injury. The dorsal and anterior directions are upwards and leftwards, respectively. In cases of successful regeneration to the ventral nerve cord (A), we label the primary axon terminus (blue circle) at the point of innervation to the ventral nerve cord, and label all other axon termini (red circles) as the ends of any other axon branches or outgrowths. In cases of unsuccessful regeneration to the ventral nerve cord (B), we label the primary axon terminus (blue circle) as the end of the longest axon shaft, and label the remaining axon termini (red circles) as the ends of any axon branches from the main shaft (e.g. the uppermost branch in B) or the ends of shorter axon shafts. (**C**) Scatter plots showing the positions of regenerated axon termini in all L3, L4 and young adult animals. In the case of young adult animals, surgery was performed shortly after the last larval molt. In the manner shown in A,B, all primary and secondary regenerating axon termini are indicated by large blue and small red circles, respectively. In order to consolidate data from different worms, all scatter plots are scaled by each worm's circumference. In each scatter plot, the top line indicates the dorsal nerve cord, the bottom line indicates the ventral nerve cord and the broken line indicates the longitudinal axis halfway between the dorsal and ventral nerve cords. The wild-type morphology of the AVM axon before surgery is drawn in green. The distance between the top and bottom lines corresponds to half of total worm circumference, and the horizontal axis shows a proportion of body length equivalent to about 3.5 circumferences. (**D**) Bar chart showing the percentage of successful ventral guidance of the regenerating AVM axons in various stage animals based on the scatter plots shown in Fig. 5C. Asterisk indicates a case in which an early developmental stage differs significantly from the young adult ($P<0.05$). (**E**) Bar charts of average axon length based on the scatter plots shown in C, scaled by worm circumference (in which 1 corresponds to half of total worm circumference) and unscaled (in μm). Axon length corresponds to the contour length between the cell body and axon termini. Asterisks indicate cases in which an early developmental stage is significantly different from the young adult ($P<0.05$). Error bars represent ±1 s.e.m.

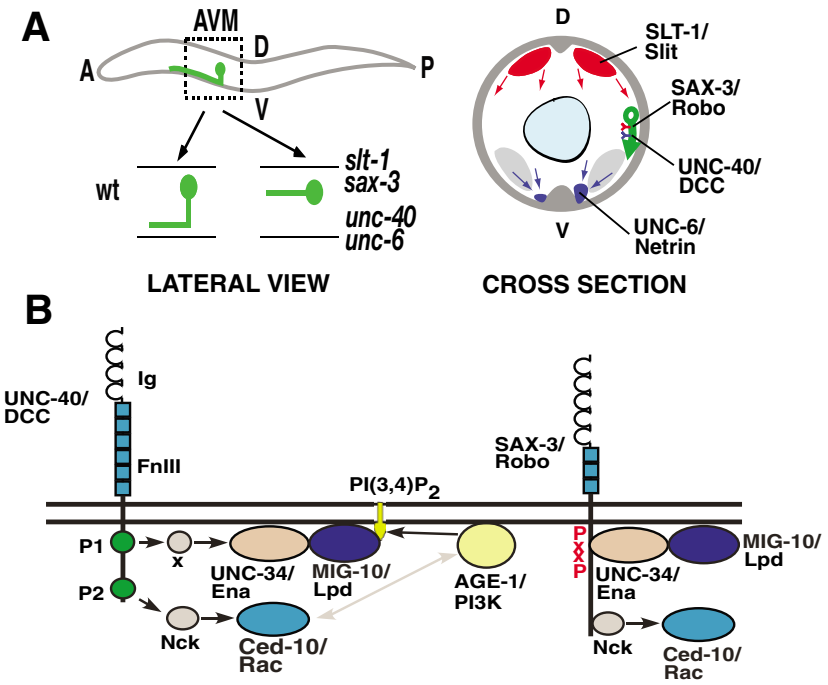

Fig. 6. Cellular and molecular determinants of initial axon development in AVM neuron. (**A**) Schematic of the axon guidance systems used by the AVM neuron during development. Dorsal muscles express the repellent SLT-1/Slit (red). Ventral axons express the attractant UNC-6/netrin (blue). (**B**) Schematic of signaling molecules that operate downstream of the guidance receptors in AVM axon development.

in L3, L4 and young adult animals (Fig. 5). We cut AVM axons halfway along their ventral projections at each developmental stage, and found that advancing development leads to significant decrease in the total amount of regenerative axonal outgrowth, as well as to a significant decrease in guidance precision to the ventral nerve cord. Taken together, these results point to significant shifts in the regenerative capacity from larval to adult stage.

Distinct molecular requirements for initial axon development and adult-stage axon regeneration

The current model for AVM axon guidance during initial development is shown in Fig. 6. Mutations in either the netrin- or slit-based guidance systems result in a 30-40% penetrant defect in AVM ventral guidance, whereas mutations in both systems lead to nearly complete failure (~90%) of ventral guidance (Hao et al., 2001; Chang et al., 2004). As the AVM neuron integrates at least two redundant guidance systems to direct its axon to the ventral nerve cord, it is possible to analyze axon guidance mutants with wild-type axon trajectories at the adult stage, to study whether specific guidance molecules affect rewiring after axotomy. In this study, we did not analyze rewiring in cases of initially aberrant axon trajectories, as pre-existing anatomical abnormalities might hinder subsequent axon regeneration. Furthermore, as developmental stage affects regenerative ability of AVM neurons, a potential problem when comparing the effects of different mutations, we carefully controlled for developmental stage by always performing femtosecond laser axotomy of AVM neurons in young adult animals shortly after they exited the last larval molt.

We found that the AVM axon in *unc-40*/DCC mutants displayed the same level of success in regenerating and reaching the ventral nerve cord after adult-stage axotomy as in wild-type worms, but was significantly less successful in *unc-6*/netrin mutants. One possibility is that *unc-6*/netrin continues to mediate guidance in the regenerating AVM axons of adult animals, but through an *unc-40*/DCC-independent mechanism (Fig. 7A,B). The *unc-5* gene encodes an alternative netrin receptor in *C. elegans*. We found that AVM axon regeneration in the *unc-5* mutants was indistinguishable from wild-type animals, suggesting that the *unc-5* receptor alone is not sufficient to mediate attraction to *unc-6*/netrin during regeneration (Fig. 7A,B). We note that *unc-6*/netrin also adopts a significant role in anteroposterior guidance of regenerating AVM axons, as we frequently observed regenerated AVM axons in *unc-6* mutants projecting extensively in the posterior direction (30%; n=23) in contrast to exclusively anterior projections in wild-type worms during initial development (Fig. 7A, Fig. 8C,D).

We found that *slt-1* continues to be expressed by dorsal body wall muscles in the adult stage (Fig. 9A) and contributes to the ventral guidance of the regenerating AVM axons. The regenerative axon guidance defect caused by *slt-1* mutation is not obvious by itself but is revealed by its enhancing the defect caused by an *unc-6* mutation (Fig. 7B). Even in the absence of SLT-1 activity, developing AVM axons never project to the dorsal midline (0%; n>100). By contrast, regenerating AVM axons frequently project to the dorsal midline (37%; n=19) (Fig. 7A, Fig. 8B). These results suggest that SLT-1 is the major axon repellent that mediates dorsal repulsion at the adult stage, whereas a redundant axon repellent cooperates with SLT-1 during early development to repel AVM axons away from the dorsal midline.

A candidate redundant repellent is UNC-129/TGF-β as UNC-129, like SLT-1, is also expressed in dorsal body wall muscles during development (Colavita et al., 1998) and an *unc-129* mutation strongly enhances the AVM axon guidance phenotypes of *slt-1* mutants (C.C., T. Yu and C. Bargmann, unpublished). UNC-129/TGF-β continues to be expressed in dorsal body wall muscles at the adult stage (Fig. 9B). However, we found that *unc-129* no longer exerts its effects on adult AVM axons, as an *unc-129* mutation does not enhance AVM regenerative phenotypes of *slt-1* mutants (Fig. 7A,B). One possible explanation is that TGF-β receptor signaling might be inactivated in adult AVM neurons. This hypothesis awaits further demonstration as the UNC-129/TGF-β receptor has not yet been identified in *C. elegans* (Colavita et al., 1998).

The signaling molecules UNC-34/Ena, CED-10/Rac and MIG-10/Lamellipodin (Lpd) operate downstream of axon guidance receptors during initial AVM axon development, forming two

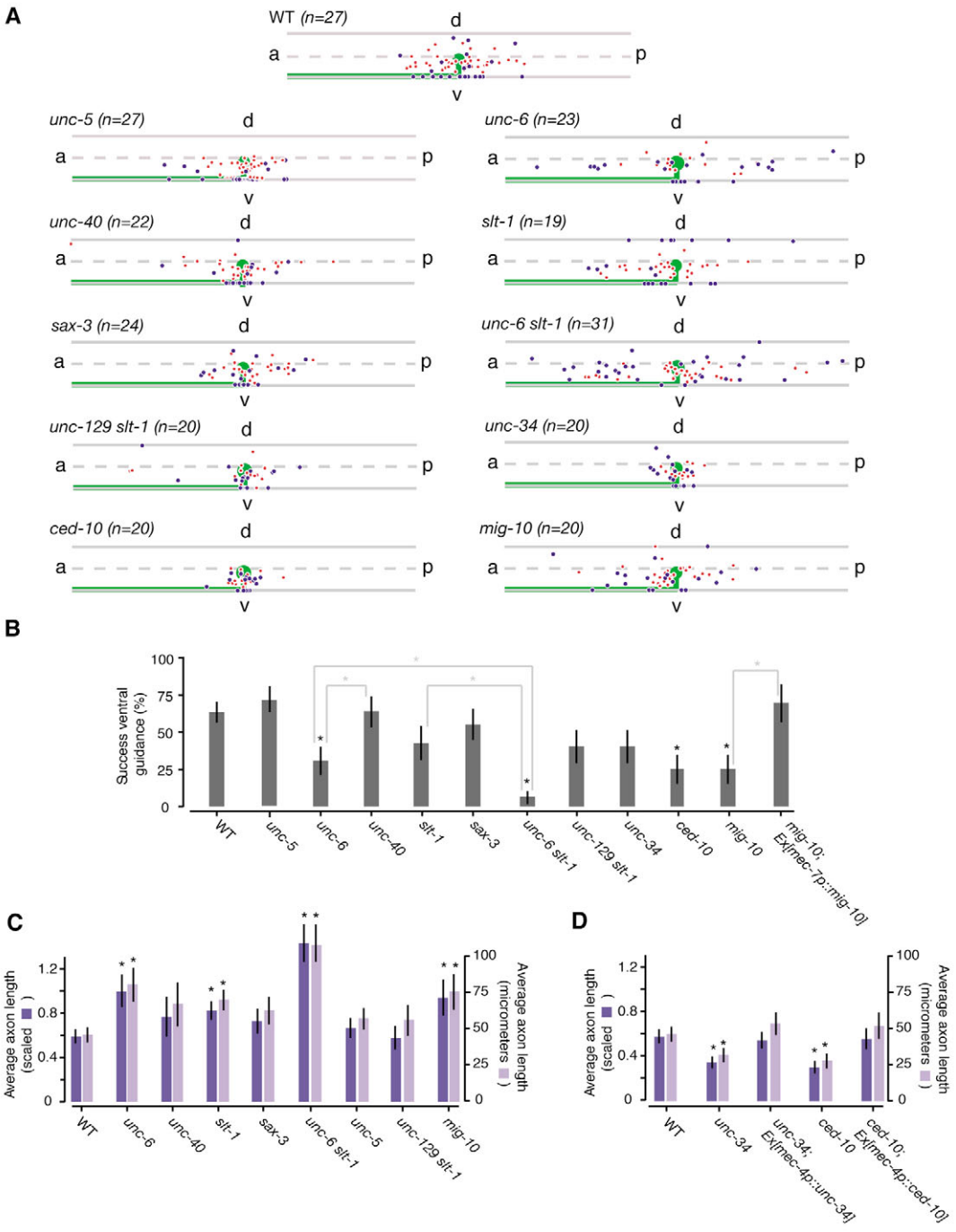

Fig. 7. Molecular requirements for regenerative axon growth and guidance. (**A**) Scatter plots (as in Fig. 5C) showing the positions of regenerated axon termini in all wild-type, *unc-6*, *unc-40*, *unc-5*, *slt-1*, *sax-3*, *unc-6 slt-1*, *unc-129 slt-1*, *unc-34*, *ced-10* and *mig-10* animals. All surgeries were performed on young adult worms, shortly after they exited the last larval molt. (**B-D**) Bar charts (as in Fig. 5D,E) showing the percentage of successful ventral guidance and average axon length of the regenerating AVM axons in wild-type and mutant worms based on the scatter plots shown in A. (B,C) Asterisks indicate cases in which mutant differs from wild-type or specific comparisons are significantly different (P<0.05). (D) Asterisks indicate cases in which mutant differs from wild-type or rescued worms (P<0.05). Error bars represent ±1 s.e.m.

redundant pathways that mediate axon guidance (Gitai et al., 2003; Lundquist et al., 1998; Chang et al., 2006; Quinn et al., 2006) (Fig. 6B). Based on inspection of AVM morphology after initial development in *unc-34(gm104)* and *ced-10 (n1993)* mutant animals (n>100), we observed normal axon outgrowth in every animal. Thus, both UNC-34/Ena and CED-10/Rac are not required for developmental axon growth. By contrast, both UNC-34/Ena and CED-10/Rac are essential for adult-stage axon regrowth (Fig. 7A,D, Fig. 8F,G). We quantified regenerative axonal outgrowth by measuring the average length along the contour of all primary and secondary regenerated axons (Fig. 5A,B). Using this metric, both *unc-34* and *ced-10* mutants exhibit stunted axonal outgrowth after adult-

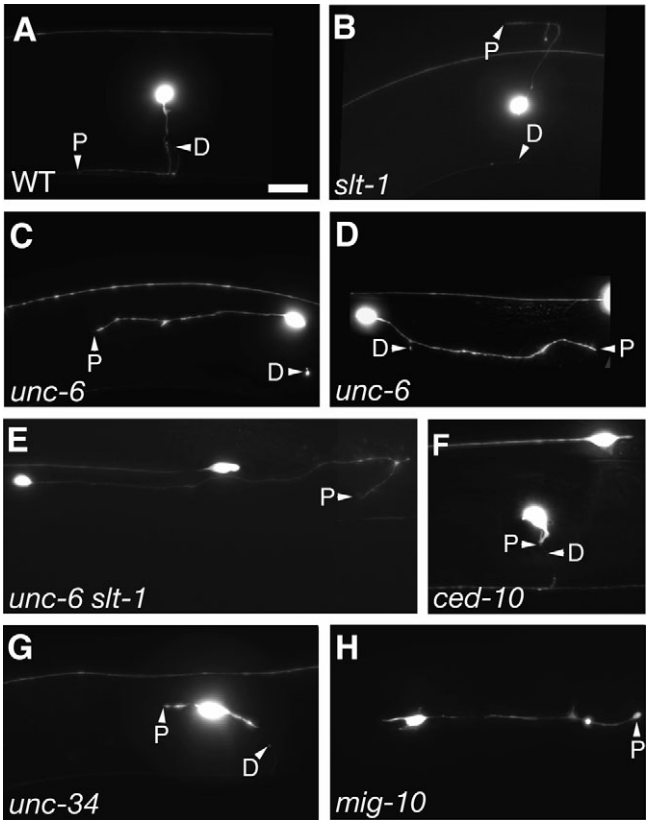

Fig. 8. Representative patterns of regenerated AVM axon in wild-type and mutant worms 24 hours after axotomy in the young adult stage. In each image, the dorsal and anterior directions are upwards and leftwards, respectively. Scale bar: 20 μm. (**A**) The wild-type regenerated axon reaches the ventral nerve cord. (**B**) The AVM axon of a *slt-1* mutant reaches the dorsal midline. Anteriorly (**C**) and posteriorly (**D**) projecting AVM axons in *unc-6*/netrin mutants. (**E**) An AVM axon in an *unc-6 slt-1* double mutant is considerably longer than in average wild-type worms. Defective axon outgrowth in *ced-10*/rac1 (**F**) and *unc-34*/Ena (**G**) mutants. (**H**) Aberrant axon rewiring in a *mig-10*/Lpd mutant.

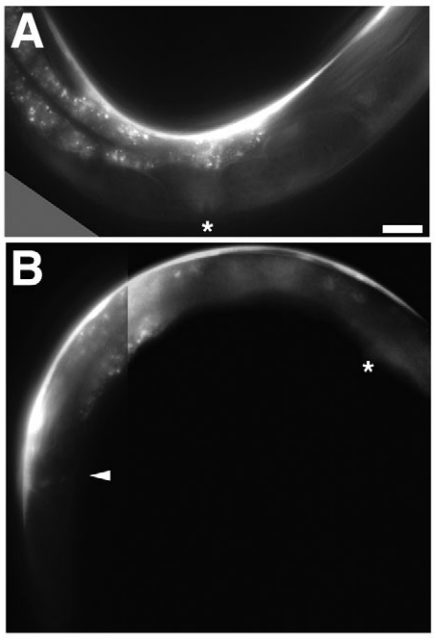

Fig. 9. Expression patterns of *slt-1*/slit and *unc-129*/TGF-β in adults. (**A**) SLT-1 maintains its expression in dorsal body wall muscles into adulthood. Only the mid-body region is shown. (**B**) UNC-129/TGF-β is expressed at high levels in dorsal body wall muscles into adulthood. Anterior to mid-body region is shown. Asterisks indicate the positions of the vulvae and the arrowhead indicates the nerve ring in the head. In each image, dorsal is upwards and anterior is leftwards. Scale bar: 50 μm.

stage axotomy, which may contribute to the poor success rate with which regenerating AVM axons in *ced-10* mutants reach the ventral midline (Fig. 7A,B). Expressing UNC-34/Ena and CED-10/Rac in the mechanosensory neurons using the cell-type specific *mec-4* promoter rescued regenerative axon outgrowth defects of *unc-34(gm104)* and *ced-10(n1993)* mutants, indicating that these molecules function cell autonomously in AVM for adult-stage axon regeneration (Fig. 7D). By the axonal length metric, the *unc-6* mutation has the interesting and quantifiable effect of enhancing regenerative axonal outgrowth, an effect that is augmented in *unc-6 slt-1* double mutants (Fig. 7A,C, Fig. 8E).

We also discovered that *mig-10*/Lpd mutants, which exhibit normal axon guidance during initial development (Chang et al., 2006; Quinn et al., 2006), exhibit more extensive adult-stage axon regrowth than wild-type animals, but less success in reaching the ventral nerve cord (Fig. 7A-C, Fig. 8H). Expressing *mig-10*/Lpd using the cell-type specific *mec-7* promoter rescues this guidance defect during regeneration in *mig-10(ct41)* mutants, suggesting that MIG-10/Lpd function cell autonomously in the AVM neurons for adult-stage axon regeneration (Fig. 7B). Taken together, our observations suggest that MIG-10/Lpd mediates regenerative axon guidance, whereas UNC-34/Ena and CED-10/Rac are required for regenerative axon outgrowth. Similar functional partitioning has been observed during initial development: MIG-10/Lpd is required for filopodia polarization, whereas UNC-34/Ena is required for filopodia formation (Chang et al., 2006).

DISCUSSION

Axon regeneration after traumatic injury of the adult nervous system is a major challenge to clinical neuroscience (Case and Tessier-Lavigne, 2005). Understanding the molecular basis for axon regeneration in different neuronal cell types and at different stages of development may be the key to advancing clinical neurology from palliative care to actual cures for victims of CNS injury. With vertebrate models such as mouse or rat, molecular factors that affect nervous system regeneration are typically identified through biochemical approaches. The development of a complementary genetic approach should facilitate the identification of new factors. The discovery that neurons in adult *C. elegans* regrow after femtosecond laser axotomy suggested that the nematode may provide a genetic model for adult-stage regeneration.

Our observations uncovered specific features of adult-stage regeneration in *C. elegans* that resemble clinically relevant features of regeneration in higher mammals. In *C. elegans*, we found that different neuronal cell types exhibit different capacities for regeneration. Neurons in the worm's head tend not to regenerate after axotomy, but neurons in the body reliably regenerate. Similarly, in mammals, neurons in the peripheral nervous system tend to regenerate after traumatic injury, but neurons in the central nervous system fail to regenerate. In *C.*

elegans, we found that axotomy at the adult stage can stimulate the formation of multiple growth cones, exploratory outgrowth and imprecise pruning of excessive outgrowths. Similarly, in mammals, exuberant axon sprouting can often be found at the sites of brain lesions, which is frequently associated with post-traumatic epilepsy. In addition, in *C. elegans*, we found that the location of the axotomy with respect to the cell body affects regeneration patterns, and that regenerative capacity is higher in early development than in adult stage. Both are well-established features of mammalian axonal regeneration.

In the case of the AVM neurons, we observed clear differences in the genetic requirements between wiring during initial development and rewiring during adult-stage regeneration. Mutations in certain genes, e.g. *unc-40*/DCC and *unc-129*/TGF-β, have significant effects on initial wiring without having significant effects on rewiring. Mutations in other genes, e.g. *ced-10*, *unc-34* and *mig-10*, have significant effects on rewiring without having significant effects on initial wiring. High-throughput methods for stereotyped femtosecond laser axotomy in *C. elegans* should enable unbiased, forward genetic screens to identify new molecules that allow the nervous system to regenerate and repair itself after traumatic injury at the adult stage.

We thank WormBase for access to *C. elegans* information; E. Mazur for sharing femtosecond laser ablation technology; C. I. Bargmann, L. Zipursky, J. R. Sanes, L. Luo, T. Clandinin, K. Shen and L. Case for helpful discussions; C. I. Bargmann, P. Sengupta and the Caenorhabditis Genetics Center for nematode strains; S. Clark for *mec-4* promoter; A. Fire for vectors; J. L. Liu, F. Xin, M. Kaikhosrovi, P. A. T. Nguyen and S. Patel for strain and plasmid constructions, microinjection, and technical support; This work was supported by grants from the McGill University Startup funds (to C.C.), and from Sloan, McKnight, Dana and National Science Foundations (to A.D.T.S.).

References

Bradke, F. and Dotti, C. G. (2000). Differentiated neurons retain the capacity to generate axons from dendrites. *Curr. Biol.* **10**, 1467-1470.

Brenner, S. (1974). The genetics of Caenorhabditis elegans. *Genetics* **77**, 71-94.

Case, L. C. and Tessier-Lavigne, M. (2005). Regeneration of the adult central nervous system. *Curr. Biol.* **15**, R749-R753.

Chang, C., Yu, T. W., Bargmann, C. I. and Tessier-Lavigne, M. (2004). Inhibition of netrin-mediated axon attraction by a receptor protein tyrosine phosphatase. *Science* **305**, 103-106.

Chang, C., Adler, C. E., Krause, M., Clark, S. G., Gertler, F. B., Tessier-Lavigne, M. and Bargmann, C. I. (2006). MIG-10/lamellipodin and AGE-1/PI3K promote axon guidance and outgrowth in response to slit and netrin. *Curr. Biol.* **16**, 854-862.

Chung, S. H., Clark, D. A., Gabel, C. V., Mazur, E. and Samuel, A. D. (2006). The role of the AFD neuron in C. elegans thermotaxis analyzed using femtosecond laser ablation. *BMC Neurosci.* **7**, 30.

Clark, D. A., Biron, D., Sengupta, P. and Samuel, A. D. (2006). The AFD sensory neurons encode multiple functions underlying thermotactic behavior in Caenorhabditis elegans. *J. Neurosci.* **26**, 7444-7451.

Colavita, A., Krishna, S., Zheng, H., Padgett, R. W. and Culotti, J. G. (1998). Pioneer axon guidance by UNC-129, a C. elegans TGF-beta. *Science* **281**, 706-709.

Dotti, C. G. and Banker, G. A. (1987). Experimentally induced alteration in the polarity of developing neurons. *Nature* **330**, 254-256.

Gitai, Z., Yu, T. W., Lundquist, E. A., Tessier-Lavigne, M. and Bargmann, C. I. (2003). The netrin receptor UNC-40/DCC stimulates axon attraction and outgrowth through enabled and, in parallel, Rac and UNC-115/AbLIM. *Neuron* **37**, 53-65.

Goslin, K. and Banker, G. (1989). Experimental observations on the development of polarity by hippocampal neurons in culture. *J. Cell Biol.* **108**, 1507-1516.

Hao, J. C., Yu, T. W., Fujisawa, K., Culotti, J. G., Gengyo-Ando, K., Mitani, S., Moulder, G., Barstead, R., Tessier-Lavigne, M. and Bargmann, C. I. (2001). C. elegans slit acts in midline, dorsal-ventral, and anterior-posterior guidance via the SAX-3/Robo receptor. *Neuron* **32**, 25-38.

Hayashi, K., Kawai-Hirai, R., Ishikawa, K. and Takata, K. (2002). Reversal of neuronal polarity characterized by conversion of dendrites into axons in neonatal rat cortical neurons in vitro. *Neuroscience* **110**, 7-17.

Knobel, K. M., Jorgensen, E. M. and Bastiani, M. J. (1999). Growth cones stall and collapse during axon outgrowth in Caenorhabditis elegans. *Development* **126**, 4489-4498.

Lundquist, E. A., Herman, R. K., Shaw, J. E. and Bargmann, C. I. (1998). UNC-115, a conserved protein with predicted LIM and actin-binding domains, mediates axon guidance in C. elegans. *Neuron* **21**, 385-392.

Mello, C. and Fire, A. (1995). DNA transformation. *Methods Cell Biol.* **48**, 451-482.

Quinn, C. C., Pfeil, D. S., Chen, E., Stovall, E. L., Harden, M. V., Gavin, M. K., Forrester, W. C., Ryder, E. F., Soto, M. C. and Wadsworth, W. G. (2006). UNC-6/netrin and SLT-1/slit guidance cues orient axon outgrowth mediated by MIG-10/RIAM/lamellipodin. *Curr. Biol.* **16**, 845-853.

Shen, N., Datta, D., Schaffer, C. B., LeDuc, P., Ingber, D. E. and Mazur, E. (2005). Ablation of cytoskeletal filaments and mitochondria in live cells using a femtosecond laser nanoscissor. *Mech. Chem. Biosyst.* **2**, 17-25.

Wadsworth, W. G., Bhatt, H. and Hedgecock, E. M. (1996). Neuroglia and pioneer neurons express UNC-6 to provide global and local netrin cues for guiding migrations in C. elegans. *Neuron* **16**, 35-46.

White, J. G., Southgate, E., Thomson, J. N. and Brenner, S. (1986). The structure of the nervous system of the nematode Caenorhabditis elegans. *Philos. Trans. R. Soc. London Ser. B* **314**, 1-340.

Wu, Z., Ghosh-Roy, A., Yanik, M.F., Zhang, J.Z., Jin, Y. and Chisholm, A.D. (2007). Caenorhabditis elegans neuronal regeneration is influenced by life stage, ephrin signaling and synaptic branching. *Proc. Natl. Acad. Sci. USA* **104**, 15132-15137.

Yanik, M. F., Cinar, H., Cinar, H. N., Chisholm, A. D., Jin, Y. and Ben-Yakar, A. (2004). Neurosurgery: functional regeneration after laser axotomy. *Nature* **432**, 822.